Fuzzy-based prediction for suddenly expanded axisymmetric nozzle flows with microjets

Jaimon D. QUADROS [1] [iD] *, Suhas P. [2], Sher A. KHAN [3] [iD], Abdul AABID [4],
Muneer BAIG [4], and Yakub I. MOGUL [5]

[1] Fluids Group, School of Mechanical Engineering, Istanbul Technical University, Gümüşsuyu, 34437 Istanbul
[2] Department of Mechanical Engineering, Sahyadri College of Engineering and Management, Mangaluru 575007, Karnataka, India
[3] Department of Mechanical Engineering, Kulliyyah of Engineering, International Islamic University Malaysia, 53100, Selangor, Malaysia
[4] Department of Engineering Management, College of Engineering, Prince Sultan University, 66833, Riyadh 11586, Saudi Arabia
[5] National Centre for Motorsport Engineering, University of Bolton, Bolton, BL3 5AB, UK

Abstract. The current research focuses on the implementation of the fuzzy logic approach for the prediction of base pressure as a function of the input parameters. The relationship of base pressure (β) with input parameters, namely, Mach number (M), nozzle pressure ratio (η), area ratio (α), length to diameter ratio (ξ), and jet control (ϑ) is analyzed. The precise fuzzy modeling approach based on Takagi and Sugeno's fuzzy system has been used along with linear and non-linear type membership functions (MFs), to evaluate the effectiveness of the developed model. Additionally, the generated models were tested with 20 test cases that were different from the training data. The proposed fuzzy logic method removes the requirement for several trials to determine the most critical input parameters. This will expedite and minimize the expense of experiments. The findings indicate that the developed model can generate accurate predictions

Key words: base pressure; Mach number; fuzzy modeling.

1. INTRODUCTION

The exhaust plumes from rockets and missile engines have proven to be a grave concern with supersonic vehicles. The outflow of air inside high-speed vehicle engines is confirmed to alleviate the base drag [1]. For instance, a nozzle equipped with rapid expansion ducts will create a recirculation zone, raising the losses. Numerous studies have shown the use of passive and active control methods to regulate high-speed flows. In the passive control approach, the geometry of the duct is altered by adding extra devices such as ribs, cavities, etc. [2]. In the case of active controls, the researchers utilized a high-speed nozzle with an expanded duct and microjet controller; a small hole is drilled in the base region to control the flow, which was proven to be an efficient approach for the supersonic flow problem [3, 4].

Base drag, caused by flow separation at the blunt base of an aerodynamic body, can account for a sizable portion of overall drag. When an abrupt change in geometry results in a separation, the flow exhibits three distinct zones: separation, recirculation, and re-attachment (Fig. 1). At the nozzle outlet, the recirculation zone generates negative pressure, referred to as base pressure. Base pressure is inversely proportional to base drag, implying that an increase in base pressure results in a decrease in base drag and vice versa. The base drag component of

a missile overall drag can be as high as 50% when the missile is powered down (i.e. with no jet flow at the base). Numerous researchers have proposed various ways of controlling base pressure using active and passive controllers, experimentally and analytically. The section below discusses works published contemporaneously with this study. The base pressure was initially investigated by Korst [1] in various Mach number regimes, with the flow exhibiting sonic and supersonic behavior at the base and wake, respectively. A physical model for base pressure was developed that analyzed the interaction between flows at the jet and wake. Khan and Rathakrishnan [2] conducted tests to determine the influence of micro-jets on the base pressure behavior of an over-inflated nozzle. Experiments were conducted by means of airflow from a settling chamber into the suddenly expanded duct through a nozzle. A blowing chamber was used to blow air in the form of microjets. The study demonstrated that base pressure was controlled effectively through the employment of micro jets. Khan and Rathakrishnan [3] conducted experiments to modify base pressure. $M = 1.87, 2.2$, and 2.58, and NPR $= 3, 5, 7, 9$, and 11, were utilized as control parameters. An increase of 95% in base pressure was achieved for various combinations of Mach numbers and NPRs. Khan and Rathakrishnan [4] investigated the control of base pressure at an under-expansion level for nozzles with Mach numbers ranging between 1.0 and 2.0. According to their findings, microjets significantly increased the base pressure for higher Mach numbers, i.e., $M \geq 1.5$. Khan and Rathakrishnan [5] investigated flow expansion for nozzles with $M = 1.25, 1.3, 1.48, 1.6, 1.8$, and 2.0, which were correctly expanded. However, in this in-

stance, the microjets had truly negligible effect on base pressure which transpired as a result of a weak wave at the nozzle exit/duct interface. Baig *et al.* [6] investigated the base pressure control via a suddenly expanded channel. Microjets were used as active controllers to regulate base pressure for this purpose. The trials were conducted for η ranging from 3 to 11. According to the study, for certain parametric combinations, a 65% rise in base pressure was achieved. The bifurcation phenomena for sudden expansion flows were demonstrated by Chiang *et al.* [7] through experiments. The instabilities caused by modifying the channel aspect ratio and the flow Reynolds number occurred at the symmetry-breaking bifurcation point. Khan *et al.* [8] used the CFD approach to model the nozzle flow based on empirical data. ANSYS fluent was used to model a 2-D transient compressible flow of air via a supersonic nozzle. A standard k-ε was used to simulate the flow process. The results obtained were benchmark results that could be used to simulate the flow at Mach numbers other than Mach 2, and also predicted shock generation in the duct [9], providing valuable information for fluid dynamics research. Semlitsch *et al.* [10] investigated double shock diamonds at the exhaust of modular convergent-divergent nozzles. These shock patterns consisted of two structures: one originating from the nozzle throat, and another from its exit. The results observed that when the two structures overlapped, it caused tremendous pressure oscillations at the exhaust, and led to the formation of shock-associated noise.
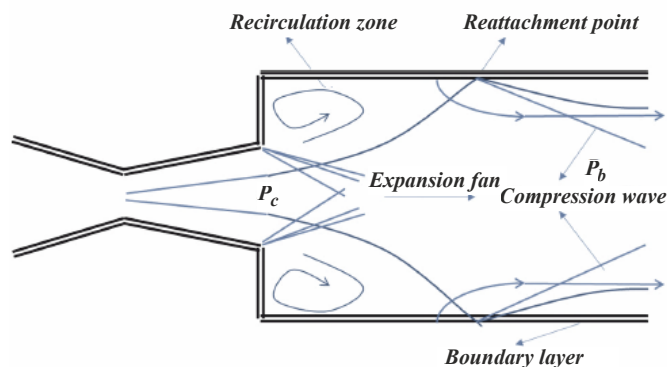

Fig. 1. Suddenly expanded flow process [2]

Soft computing and statistical analysis are novel approaches for this kind of research. It is compared to the remarkable capacity of the human mind to study in an unpredictable and imprecise environment. Quadros *et al.* [11] employed an L_9 orthogonal array to estimate base pressure using the design of experiments method. The control parameters were M, ξ, and α. The created regression models effectively predicted base pressure with high accuracy. Aabid and Khan [12] conducted experiments for these flows with and without microjets, at $M = 1.87, 2.2$, and 2.58, $\alpha = 3.24$, and ξ ranging from 10 to 1. The experimental findings were analyzed using an L_9 orthogonal array, multiple linear regression analysis, and confirmation tests. The models were statistically appropriate and capable of making good predictions in both instances. Additionally, a CFD technique was used to verify the experimental data.

The simulation results were analyzed using the k-ε turbulent model. According to the findings, (ξ) had the most significant effect on the maximum increase or decrease of base pressure. Quadros *et al.* [13] developed a prediction model for base pressure through the Artificial Neural Network (ANN) approach. The dataset used to train the network was created using the CFD technique. The ANN design consisted of three layers, with the hidden layer containing eight neurons. The ANN accurately predicted base pressure with a regression coefficient (R^2) of less than 0.99, and a root mean square error (RMSE) of 0.0032. Jagannath *et al.* [14] pioneered fuzzy logic to investigate pressure loss in a rapid expansion duct. As demonstrated by the fuzzy logic formulation, the authors sought to detect a small pressure drop when the ξ was 1. According to the authors, this was accomplished by conducting a qualitative evaluation of internal fluid flow through a nozzle equipped with a sudden expansion duct utilizing the fuzzy logic technique. Quadros *et al.* [15] discussed the vital elements of fuzzy logic technology as a cost-effective tool for the turbulent supersonic computation process. The Mamdani-based fuzzy logic approach was used to link the input and outputs of the CFD findings. This approach made use of triangular, generalized bell, and Gaussian MFs. A reasonable percentage deviation of around 9.07 % was observed. Afzal *et al.* [16] constructed six back-propagation neural network models (BPMs) to forecast pressure in high-speed flows depending on input and output variables. The data visualization revealed "η" having the most significant influence on base pressure. Six BPMs with two hidden layers, each containing four neurons, were identified to be best suited for regression analysis. BPM 5 and 6 successfully forecasted the non-linear base and wall pressure data. The L_{27} orthogonal array was used to optimize base pressure (Jaimon *et al.* [17]). A non-linear regression model for β was developed using the central composite design (CCD) and Box-Behnken design (BBD). The significance of linear, non-linear, and interaction factors in the models was determined using the ANOVA (analysis of variance). It is worth noting that several authors have successfully deployed different analyses for modifying base drag, demonstrating their effectiveness as a cost-effective tool for modeling and analyzing complex fluid flow processes. In addition to the papers mentioned above, for our study, the works of Afzal *et al.* [18–23] on clustering and regression techniques, support vector algorithms, deep neural networks, and back propagation neural network algorithms have been considered.

Most of the research to date focused on base pressure prediction through experiments and CFD simulations. Base pressure analysis using fuzzy logic-based approaches is rarely reported. Also, the use of an adaptive neuro-fuzzy system (ANFIS) for predicting base pressure is considered to be the innovative step of this research. Therefore, the current work aims to predict base pressure using a fuzzy logic approach based on the Takagi and Sugeno model. This approach uses an ANFIS and is concerned with the self-evolution of the consequent and antecedent parameters. It should be emphasized that the fuzzy approach employed both linear and non-linear MFs. The performance of the model is compared with randomly generated experimental (β) data. The research results of this study could

be used for predicting and controlling the base pressure without actually performing any experiments or simulations. The applications of this research include the design of combustion chambers and chemical reactors, where there is a requirement to decrease base pressure to enhance mixing levels, and the design of aerodynamic vehicles viz., missiles, rockets, etc., where an increment in base pressure is required for reducing base drag.

2. EXPERIMENTAL DETAILS

2.1. Experiments

Khan *et al.* [2, 3] determined the base pressures in the expanded duct by varying the geometrical and flow parameters of the convergent-divergent (C-D) nozzle. Mach numbers for these nozzles fluctuate in the supersonic range. A typical C-D nozzle of Mach 3.0 along with the enlarged duct is shown in Fig. 2a. The exit diameter of the nozzle may be maintained constant while fabricating a C-D nozzle, as the base pressure findings for nozzles with an exit diameter are available in the literature [2–5]. The isentropic relations were used to compute the throat diameter [13]. After fabrication, the nozzles are calibrated to determine the precise Mach number at the nozzle exit [13].
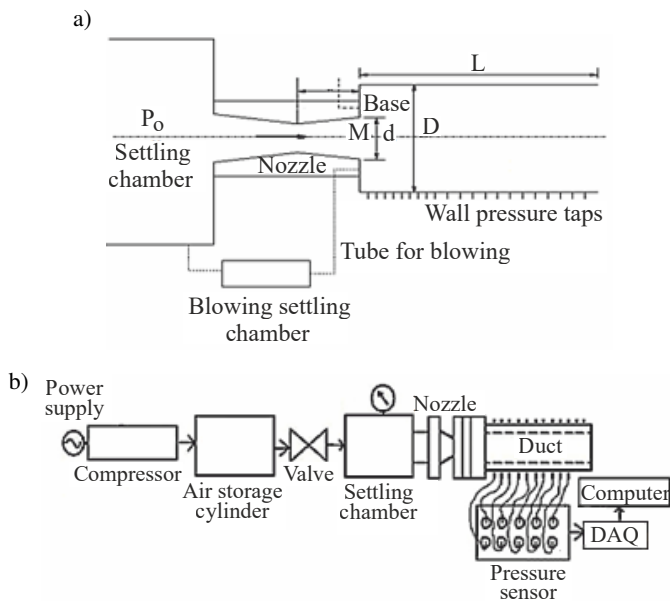
a)

b)

Fig. 2. a) Nozzle connections with the settling chamber and duct; b) data acquisition system for base pressure through the expanded duct

Figure 2b shows the complete experimental setup with the data acquisition system. There were eight holes in the outlet periphery of the nozzle, four of which were used for blowing (c), and four of which were used to determine the base pressure. The base pressure was controlled via control holes (c) which are connected to the settling chamber [4, 5]. The experiments were performed on a suddenly expanded duct having a specified (ξ). For the pressure tap location, the first nine holes (for tapping) are made at an interval of 3 mm each and the remaining are made at an interval of 5 mm each on the en-

larged duct. The nine holes ensure proper measurement of recirculation pressure or base pressure as they are in the vicinity of the nozzle exit. The base pressure and pressure in the settling chamber were measured using a PSI model 9010 pressure transducer. It measures pressures between 0 and 300 psi. The measurements are averaged and represented at a rate of 250 samples per second. User-friendly software was used to connect the computer and the transducer. The software collects the output data from all measurement channels and presents it on the computer screen concurrently. The transducer had a resolution of ± 0.003 and a reading accuracy of up to $\pm 1\%$. The input and output variables for the suddenly expanded flow process are shown in Fig. 3. All the non-dimensional base pressure presented in this paper is within an uncertainty band of $\pm 2.6\%$.
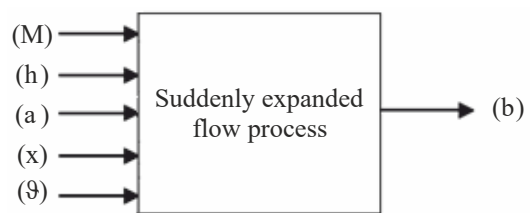

Fig. 3. Input output for suddenly expanded flow process

2.2. Data collection

In artificial intelligence approaches, the performance of the created models is dependent on the quality and quantity of training data employed. In soft computing applications, training must be conducted using a large (say, 500) data set, which contains all conceivable permutations of input variables and their ranges. Collecting such data through genuine trials is time intensive and impractical since it results in significant material wastage, labor, and time consumption [24]. A massive amount of training data was randomly produced using the response equation [24]. The response equation (input-output relationship) for the present study was developed using the DoE-based L_{16} Orthogonal array [25], comprising five factors at levels as shown in Table 1. The response equation was developed using the statistical Minitab 20 software. The parameter and level selection were done after conducting trial experiments. Additionally, the data utilized to evaluate the models were gathered via experiments and were not used to train the FLC. A response/regression equation for (β), as a function of flow and geometric parameters, is illustrated by Equation (1). The regression equation was tested

Table 1
Suddenly expanded flow parameters and levels

Parameters	Notation	Level 1	Level 2
M	A	2.0	3.0
η	B	3	7
α	C	4.75	6.25
ξ	D	4	8
ϑ	E	1 (without control)	2 (with control)

J.D. Quadros, Suhas P., S.A. Khan, A. Aabid, M. Baig, and Y.I. Mogul

for accuracy with the help of 20 random experimental test cases (Table 2) and obtained a prediction accuracy of $\pm 6.52\%$.

$$
\begin{aligned}
\beta = {} & 079 + (0.712 \times A) + (0.023 \times B) + (0.401 \times C) \\
& - (0.315 \times D)(0.0209 \times E) + (0.319 \times A \times B) \\
& + (0.201 \times B \times C) - (0.122 \times C \times D) \\
& + (0.0137 \times D \times E) + (0.0137 \times A \times B \times C \times D \times E).
\end{aligned}
\tag{1}
$$

Table 2
Random experimental test cases

Exp. no.	Input					Output
	M	H	α	ξ	Θ	β
1	2.0	A	4.75	4	1	0.234
2	2.5	3	6.25	5	2	0.443
3	3.0	5	6.25	6	2	0.229
4	2.0	5	6.25	7	2	0.678
5	3.0	7	6.25	8	1	0.656
6	2.5	7	6.25	6	1	0.737
7	3.0	5	6.25	7	1	0.441
8	2.5	7	6.25	4	2	0.666
9	2.0	5	4.75	6	2	0.921
10	3.0	7	4.75	7	1	0.990
11	2.5	3	4.75	8	2	0.721
12	2.5	3	4.75	8	1	0.844
13	3.0	7	4.75	4	2	0.225
14	3.0	7	4.75	4	1	0.449
15	3.0	7	6.25	5	2	0.557
16	2.0	5	4.75	5	1	0.698
17	2.5	5	6.25	6	2	0.361
18	2.0	5	4.75	6	2	0.551
19	2.0	3	4.75	7	1	0.328
20	2.5	5	6.25	7	2	0.751

2.3. Fuzzy modeling

Modeling is the process of discovering, analyzing, and verifying the input-output connections of a physical system. The fuzzy approach is utilized to create the link between the input variables of the flow process and the base pressure [26]. Fuzzy modeling is used in the present study to predict the output (β), given the set of inputs (M, η, α, ξ, and ϑ) are known. For this purpose, the Takagi and Sugeno-based model has been used. Linear and non-linear (Triangular and Generalized bell shape and Gaussian) MF distributions, along with twenty random test cases (see Table 2) were utilized to evaluate the model performance. In Fig. 4, we can see the input-output model of the flow process, which uses fuzzy logic.

3. FUZZY LOGIC CONTROLLER

Due to the accelerated advancement of fuzzy logic applications to complicated real-world situations, researchers/investigators are more intrigued to develop fuzzy-based input-output connections. Creative explanation based on human thinking and reasoning is utilized to create the links between the input and output of the system. Fuzzy logic has three main advantages: it is easy to comprehend, it can deal with ambiguity, and does not require an exact mathematical formulation [26, 27].

In fuzzy logic, the effectiveness of the model depends on the knowledge base composed of a database and a rule base [27]. The MF is determined in a database that depends on the dispersed data of process variability. Linear type distributions represent the Trian-gular and Trapezoidal MFs, whereas non-linear data distributions include bell shape, sigmoid, and Gaussian MFs [28]. In fuzzy logic systems, variables are described using language words such as low, medium, high, tiny, etc. The input-output connections are stated using rules as functions of the linguistic terms [27, 28]. The number of rules varies as per linguistic terms and process variables used.

3.1. Takagi Sugeno's approach

Artificial neural networks (ANN) are a great and cost-effective technique for modeling complicated industrial processes [29]. The explanation for this might be because they have enhanced learning skills and the ability to generalize (predict appropriate output for inputs that are not utilized during the learning phase) [30]. A few drawbacks of ANN include the following: output precision is restricted, solutions become trapped in local minima, massive data covering the whole range of process variables is required to train the network, and a large number of training epochs [31, 32].

Wong and Lai [33] demonstrated that fuzzy ideas may be successfully applied to challenges in various mechanical engineering aspects. The primary advantages of the fuzzy logic method include increased formulation flexibility and the capacity to deal with imprecise input-output data. It is critical to highlight that the lack of a systematic process for defining the MF distributions is the primary constraint in the fuzzy logic system [33]. In recent years, research has focused on developing hybrid systems that combine the beneficial characteristics of ANN and fuzzy logic tools to tackle complex real-world issues. The embedded hybrid system was created to balance the shortcomings of one soft computing tool with the advantages of the other. A hybrid system called an adaptive neuro-fuzzy interface system (ANFIS) has sufficient characteristics that include effortless implementation, improved efficiency, explicit training, exceptional characterization through fuzzy rules, and the capacity to solve complicated issues by combining numerical and linguistic skills [31, 32]. In ANFIS, ANN coupled with a fuzzy system is utilized to update the rule base automatically. Here, a hybrid learning method which includes gradient descent and least squares estimator is used to map the input and output combinations with ANFIS.

Two parameters govern the fuzzy rule, i.e., (i) the antecedent that consists of MFs and its forms, and (ii) the consequent that consists of a conditional variable associated with the input sig-

4

Bull. Pol. Acad. Sci. Tech. Sci., vol. 70, no. 5, p. e142654, 2022

nal, necessary for characterizing the network output. Hybrid learning algorithms require both forward and backward computations during training. The antecedent parameters are first fixed in forward computing, and the consequent parameters are found using the least-squares method. The network output is determined by summing the outputs of subsequent layers. It should be emphasized that the primary goal of any training method is to minimize the error (between the actual and projected values), which requires updating the network parameters and is achieved via backward pass computation. The following parameters are fixed, and the premise parameters are updated using the gradient descent technique [33]. The procedures used in the current effort to create the ANFIS model are projected in Fig. 4.

Figure 5 illustrates the construction of ANFIS for the suddenly expanded flow process [28]. The network has circular and rectangular symbols that represent fixed and flexible nodes, respectively. The network design is similar to ANN, including input, output, and hidden layers. The suddenly expanded flow process parameters are declared as a function of input nodes associated with the input layer, and base pressure (β) is nominated as the output node. The nodes that operate in the hidden layer include performing MFs and rules as well. There are five input parameters and one output parameter in this study. There are 243 possible rule configurations for each of the 3 different input parameters. Equations (2), (3), and (4) for Takagi and Sugeno's first-order model, demonstrate a conventional outcome with 3 fuzzy rules.
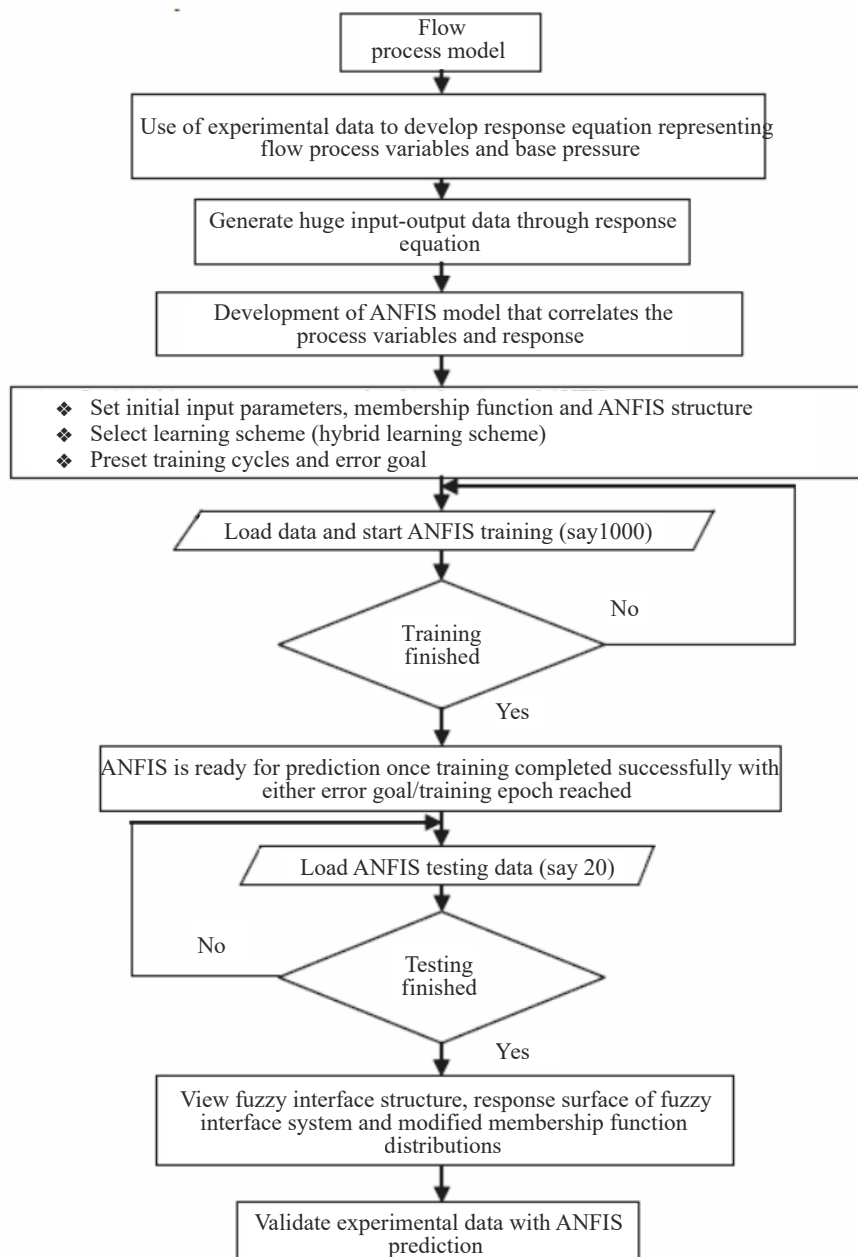

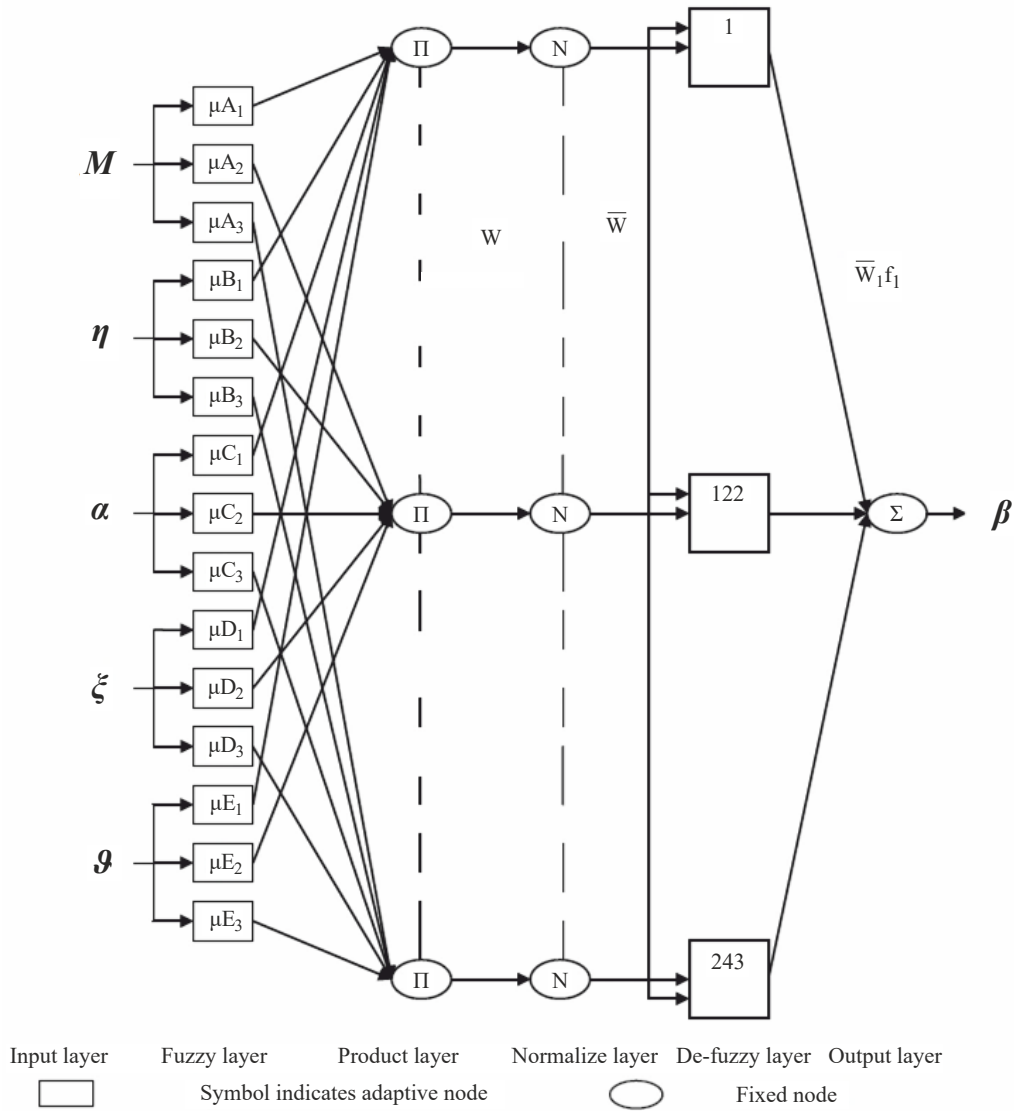**Fig. 4.** Flow chart representing methodologyfollowed for predicting (β) using ANFIS.

Bull. Pol. Acad. Sci. Tech. Sci., vol. 70, no. 5, p. e142654, 2022

5

J.D. Quadros, Suhas P., S.A. Khan, A. Aabid, M. Baig, and Y.I. Mogul

Fig. 5. ANFIS architecture for predicting (β) [34]

Rule 1: if (M is A_1), (η is B_1), (α is C_1), (ξ is D_1), and (ϑ is E_1) then

$$f_1 = p_1 M + q_1 \eta + r_1 \alpha + s_1 \xi + t_1 \vartheta + u_1 . \tag{2}$$

Rule 2: if (M is A_2), (η is B_2), (α is C_2), (ξ is D_2), and (ϑ is E_2) then

$$f_2 = p_2 M + q_2 \eta + r_2 \alpha + s_2 \xi + t_2 \vartheta + u_2 . \tag{3}$$

Rule 3: if (M is A_i), (η is B_i), (α is C_i), (ξ is D_i), and (ϑ is E_i), then

$$f_i = p_i M + q_i \eta + r_i \alpha + s_i \xi + t_i \vartheta + u_i , \tag{4}$$

where, $i = 1, 2, 3, \ldots, 243$, p_i, q_i, r_i, s_i, t_i, and u_i, are the consequent parameters, and f is the output parameter. The language terms employed to describe the MFs are A_i, B_i, C_i, D_i, and E_i.

The ANFIS structure is composed of six layers: the input layer, the fuzzification layer, the product layer, the normalization layer, the defuzzification layer, and the output layer. Setting

up an input-output connection and verifying the proper functioning of each layer is done in the following manner:

Layer 1: Suddenly expanded flow variables are described as a function of the input layer nodes in layer 1. Using a linear transformation function, layer 1 transfers the identical input data to the subsequent layer.

Layer 2 is the fuzzification layer, wherein the MF weights correlating to the prescribed linguistic labels are calculated as indicated in Equations (5)–(9). In this layer "μ" represents the fuzzification factor that transforms the input quantity into a fuzzy quantity. These are values that lead the variables to be represented by an MF due to their fuzzy nature. M, η, α, ξ, and ϑ are the input nodes represented in relation to MFs as A_i, B_i, C_i, D_i, and E_i of layer 2, where $O_{2,i}$ is the output of ith node of layer 2.

$$O_{2,i} = \mu A_i(M) \qquad \text{for } i = 1, 2, 3, \tag{5}$$
$$O_{2,i} = \mu B_{i-3}(\eta) \qquad \text{for } i = 4, 5, 6, \tag{6}$$

6

Bull. Pol. Acad. Sci. Tech. Sci., vol. 70, no. 5, p. e142654, 2022

$$O_{2,i} = \mu C_{i-6}(\alpha) \qquad \text{for } i = 7, 8, 9, \qquad (7)$$

$$O_{2,i} = \mu D_{i-9}(\xi) \qquad \text{for } i = 10, 11, 12, \qquad (8)$$

$$O_{2,i} = \mu E_{i-12}(\vartheta) \qquad \text{for } i = 13, 14, 15. \qquad (9)$$

The most frequently used MFs are triangular, generalized bell shape, and Gaussian, with values typically around zero to one, in order to match the input requirements.

Layer 3: It is often called the product layer; this layer generates the total number of potential rules ($3^5 = 243$); layer 3 has 243 nodes and is typically labeled with the word. There will be 32 functional nodes for each group of input data, with every node indicating a possible input parameter combination. Layer 2 receives the data and develops the result by multiplying all input signals, as stated in Equation (10)

$$O_{3,i} = w_i = \mu A_i(M) \times \mu B_{i-3}(\eta) \times \mu C_{i-6}(\alpha) \times$$
$$\mu D_{i-9}(\xi) \times \mu E_{i-12}(\vartheta). \qquad (10)$$

Layer 4: It is often referred to as the normalization layer, and the nodes included inside it are typically labeled as N. Its primary job is to standardize the weight functions by utilizing Equation (11). The ratio of the intensity of i-th rule firing to all other rules is calculated as the output of each node

$$O_{4,i} = \overline{w}_i = \frac{w_i}{(w_1 + w_2 + w_3 + \cdots + w_{243})}. \qquad (11)$$

Layer 5: This layer is called the defuzzification layer. In order to calculate each node, Equation (12) is used to combine all of the standard firing intensities with the outcome of the associated fired rule. For every set of the specified input parameter, there are 32 nodes in Layer 5, giving a total of 243 nodes

$$O_{5,i} = \overline{w}_i f_i \overline{w}_i (p_i M + q_i \eta + r_i \alpha + s_i \xi + t_i \vartheta + u_i). \qquad (12)$$

Layer 6: The output layer has only one variable of interest in this study, hence, has only one node. As stated in equation (13), the output is computed by combining all the input signals from layer 5

$$O_{6,i} = \sum_i \overline{w}_i f_i = \frac{\sum_i w_i f_i}{\sum_i w_i}. \qquad (13)$$

4. RESULTS AND DISCUSSION

The ability of the proposed models to predict (β) in suddenly expanded flows was evaluated using 20 randomly generated tests. This section discusses the acquired results and compares the generated model performance to experimental values. The procedure for predicting (β) using the ANFIS model has been illustrated earlier in Fig. 5. It had a significant number of training data (say 500) and was created arbitrarily using the response Equation (1). Five input parameters (M, η, α, ξ, ϑ), and a single output parameter (β) have been taken into consideration in order to develop an input-output relationship for the suddenly expanded flow process using the ANFIS model. As described

earlier, both linear (triangular) and non-linear (generalized bell shape and Gaussian) MFs were utilized. Table 2 presents the input-output data for 20 different flow process conditions. It is critical to note that the prediction accuracy of the model depends on the agreement between predicted and actual values during training and is often expressed as root mean squared error (RMSE). Figure 6 illustrates the RMSE achieved after training for various MFs for the output base pressure (β).
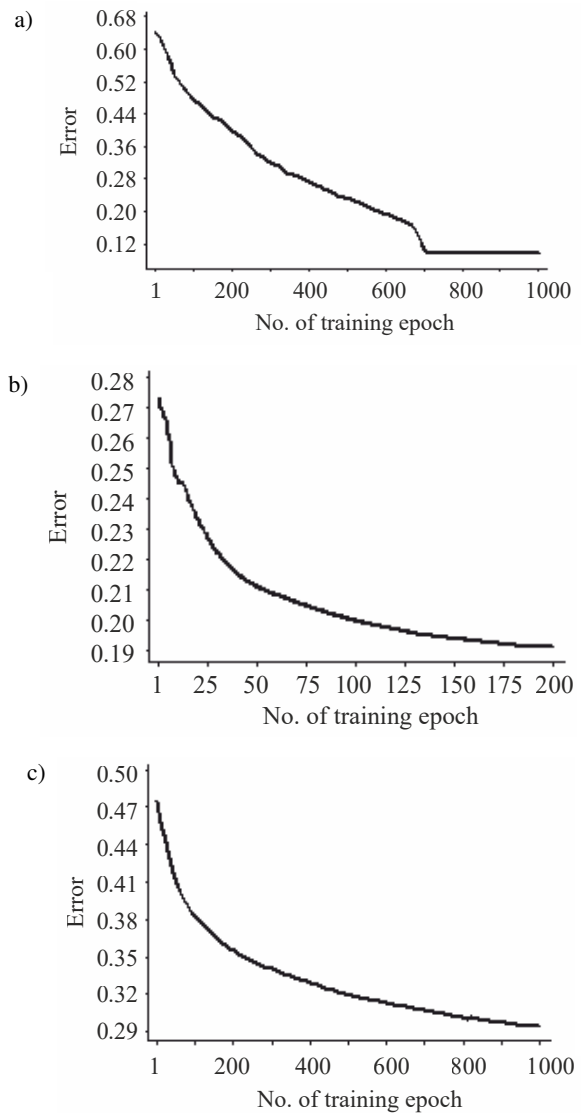

Fig. 6. Rate of convergence for the response (β) for (a) Triangular MF, (b) Bell shape MF, and (c) Gaussian MF

4.1. Comparison of membership functions

In ANFIS, ANNs are used to take fuzzy inputs, process them, and produce fuzzy outputs. ANNs are used in this technique to design the ANFIS structure automatically and configure the fuzzy parameters, rule base, database, and MFs. The efficiency of the model may be further improved by including alternative MF distributions [32, 33]. Additionally, the performance of the developed models is dependent on the volume and the nature of the training data, the degree of correlation between

Bull. Pol. Acad. Sci. Tech. Sci., vol. 70, no. 5, p. e142654, 2022

7

J.D. Quadros, Suhas P., S.A. Khan, A. Aabid, M. Baig, and Y.I. Mogul

actual and predicted values and is often assessed using the RMSE after training. For training, 500 samples of input-output data were used, and the network was terminated once the error achieved a steady state. The RMSE values obtained after training are 0.1562, 0.2842, and 0.2921 for triangular, generalized bell shape, and Gaussian MFs, respectively.

In Fig. 7, the model performance is compared with experimental test scenarios from Table 2. To match the model-predicted and actual (β) values, the best fit line was used. The optimal fit line appeared to be identical for all models. However, the triangle MF (Fig. 7a), performed better than the generalized bell shape and the Gaussian MF distribution as illustrated in Figs. 7b and 7c, respectively. This was due to the bulk of the data points in the triangular MF, lying closer to the ideal ($y = x$) line. Table 3 summarizes the results of the test scenarios for (β)

prediction. Additionally, the model performance is assessed using mean absolute percent error (MAPE) [28] values for twenty experimental test cases. The MAPE values for triangular, generalized, and Gaussian MFs distributions were 3.019, 5.998, and 6.810, respectively (Table 3).

4.2. Comparison of the MFs using percent deviations
The percent deviation in predicting (β) values for triangular MF distribution was found to be between (–4.09%, +11.96%).

Similarly, for the generalized bell shape and Gaussian MF distributions, the percent deviation in prediction values varied between (–11.177%, +8.618%), and (–8.889%, +13.456%), respectively. It is noticed that the percent deviation profile is consistent across all three models with various MF distributions; see Fig. 8.

Table 3
Random experimental test cases

Exp. No.	Actual (β)	Membership function					
		Triangular		Bell shape		Gaussian	
		Predicted (β)	Absolute deviation (%)	Predicted (β)	Absolute deviation (%)	Predicted (β)	Absolute deviation (%)
1.	0.234	0.230	1.739	0.239	2.092	0.242	3.305
2.	0.443	0.459	3.485	0.464	4.525	0.475	6.736
3.	0.229	0.220	4.090	0.220	4.090	0.226	1.327
4.	0.678	0.704	3.693	0.639	6.103	0.718	5.571
5.	0.656	0.699	6.151	0.705	6.950	0.709	7.475
6.	0.737	0.730	0.958	0.750	1.733	0.701	5.135
7.	0.441	0.455	3.076	0.420	5.000	0.405	8.888
8.	0.666	0.659	1.062	0.621	7.246	0.615	8.292
9.	0.921	0.891	3.367	0.880	4.659	0.871	5.740
10.	0.990	0.991	0.100	0.969	2.167	0.977	1.330
11.	0.721	0.733	1.637	0.789	8.618	0.779	7.445
12.	0.844	0.845	0.118	0.899	6.117	0.914	7.658
13.	0.225	0.230	2.173	0.208	8.173	0.235	4.255
14.	0.449	0.510	11.96	0.488	7.991	0.515	12.81
15.	0.557	0.581	4.130	0.501	11.17	0.620	10.16
16.	0.698	0.707	1.272	0.760	8.157	0.630	10.79
17.	0.361	0.381	5.249	0.331	9.063	0.335	7.761
18.	0.551	0.539	2.226	0.514	7.198	0.598	7.859
19.	0.328	0.338	2.958	0.358	8.379	0.379	13.45
20.	0.751	0.744	0.940	0.747	0.535	0.748	0.401
MAPE		3.019		5.998		6.819	

8

Bull. Pol. Acad. Sci. Tech. Sci., vol. 70, no. 5, p. e142654, 2022
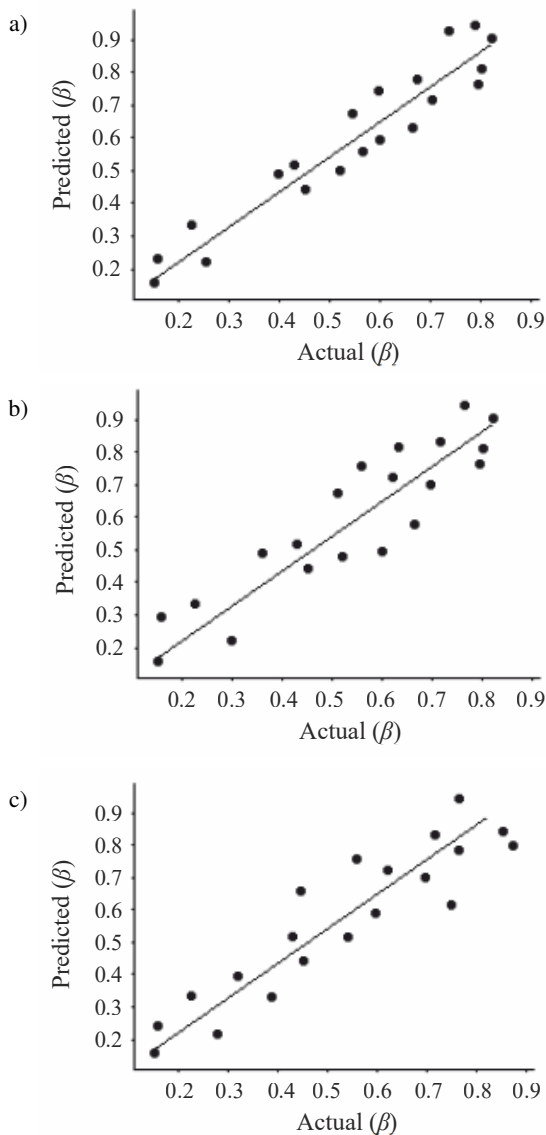
a)

b)

c)

Fig. 7. Comparison of predicted and actual (β) for (a) Triangular MF, (b) Bell shape MF, and (c) Gaussian MF

4.3. Comparison of the membership functions using MAPE

The predictive effectiveness of the developed model was tested using MAPE for three distinct MF distributions, as seen in Table 3. However, it was found that the performance differs with linear and non-linear type MF distributions, which could be accounted for by the structure of the error surface used during training [28]. The triangular MF distributions outperformed all other models in terms of MAPE. The enhanced performance of linear type MF distributions might be attributed to the automated development of the antecedent and consequent parameters of the fuzzy logic system via the enhanced learning capabilities of ANN [28, 29].

5. CONCLUSIONS

A forward mapping technique was used to estimate (β) in suddenly expanded flows by utilizing the Takagi Sugeno models' (ANFIS) based on the fuzzy logic approach. The batch training method has been used for improved training and prediction accuracy, together with a large training data set (say 500). Through genuine trials, massive databases are hard to acquire, and hence, data were produced randomly from the parameters and their levels, using the response equation developed from the DoE-based L_{16} Orthogonal array. Twenty randomly generated test cases were utilized to evaluate the performance of the model with linear and non-linear type MF distributions. It is found that the triangular MF, Bell shape MF, and Gaussian MF had a MAPE of 3.019, 5.998, and 6.819, respectively. The enhanced prediction performance of the triangular MF is mainly dependent on the quality and quantity of the training data, the distribution of MFs, and the shape of the error surfaces. The proposed fuzzy logic models may be utilized to accurately estimate base pressure under various suddenly expanded flow process conditions, therefore avoiding the need for significant experimental effort. The current work is critical for aerodynamic engineers because it identifies the most important criteria for achieving the desired base drag in the suddenly expanded flow process.
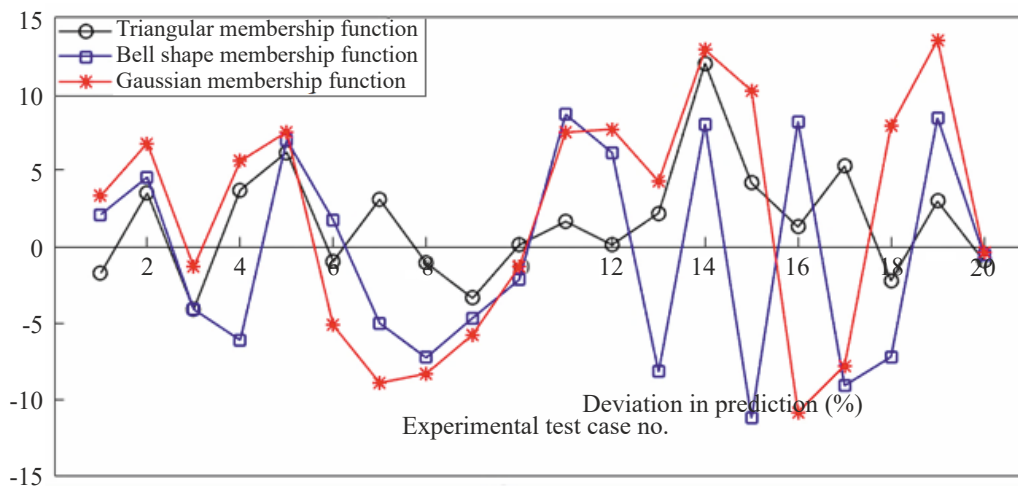

Fig. 8. Suddenly expanded flow process [2]

Bull. Pol. Acad. Sci. Tech. Sci., vol. 70, no. 5, p. e142654, 2022

9

J.D. Quadros, Suhas P., S.A. Khan, A. Aabid, M. Baig, and Y.I. Mogul

Nomenclature

A	–	linguistic label representing the Mach number in the fuzzy layer
ANFIS	–	adaptive network-based fuzzy interface system
ANN	–	artificial neural networks
ANOVA	–	analysis of variance
B	–	linguistic label representing nozzle pressure ratio in the fuzzy
BBD	–	Box-Behnken design
BPM	–	back propagation neural network models
C	–	linguistic/language label representing area ratio in the fuzzy layer
C-D	–	convergent-divergent
CCD	–	central composite design
CFD	–	computational fluid dynamics
D	–	linguistic label representing length to diameter ratio in the fuzzy
DoE	–	Design of Experiments
E	–	linguistic label representing jet control in the fuzzy layer
f	–	representation of the output parameter as per Takagi and Sugeno's first-order model
FLC	–	fuzzy logic controller
M	–	Mach number
MAPE	–	mean absolute percentage error
MF	–	membership functions
MSE	–	mean squared error
O	–	output of a particular layer in the ANFIS architecture
p	–	parameter representing the Mach number in the de-fuzzy layer
q	–	parameter representing nozzle pressure ratio in the de-fuzzy layer
$R2$	–	regression coefficient
RNN	–	recurrent neural networks
RSM	–	response surface methodology
RMSE	–	root mean square error
r	–	parameter representing area ratio in the de-fuzzy layer
s	–	parameter representing length to diameter ratio in the de-fuzzy
t	–	parameter representing jet control in the de-fuzzy layer
w	–	weight functions

Greek symbols

α	–	area ratio
β	–	non-dimensional base pressure
η	–	nozzle pressure ratio
ξ	–	length to diameter ratio
ϑ	–	jet control
μ	–	fuzzification factor

ACKNOWLEDGEMENTS

REFERENCES

[1] H.A Korst, "Theory of base pressure in Transonic and Supersonic flow," *J. Appl. Mech.*, vol. 23, pp. 593–600, 1956.

[2] A.K. Perumal, H. Singh, and E. Rathakrishnan, "Passive control of coaxial jet with supersonic primary jet and sonic secondary jet," *Phys. Fluids.*, vol. 32, p. 076101, 2020.

[3] D. Fontanarosa, M.G. De Giorgi, and A. Ficarella, "Thrust Augmentation of Micro-Resistojets by Steady Micro-Jet Blowing into Planar Micro-Nozzle," *Appl. Sci.*, vol. 11, p. 5821, 2021.

[4] B. Semlitsch, M. Mihaescu, L. Fuchs, and E.J. Gutmark, "Large Eddy Simulations of Microjets Impact on Supersonic Jet Exiting a C-D Conical Nozzle," *Am. Inst. Astronaut. Aeronaut. J.*, p. 2139, 2013, doi: 10.2514/6.2013-2139

[5] S.A. Khan and E. Rathakrishnan, "Active control of suddenly expanded flow from under expanded nozzles," *Int. J. Turbo Jet Engines*, vol. 21, no. 4, pp. 233–253, 2004.

[6] S.A. Khan and E. Rathakrishnan, "Control of suddenly expanded flow from correctly expanded nozzles," *Int. J. Turbo Jet Engines*, vol. 21, no. 4, pp. 255–278, 2004.

[7] M.A.A. Baig, F. Al-Mufadi, S.A. Khan, and E. Rathakrishnan, "Control of base flows with micro jets," *Int. J. Turbo Jet Engines*, vol. 28, no. 1, pp. 259–269, 2011.

[8] T.P. Chiang, A. Sau, and R.R. Hwang, "Asymmetry and bifurcations in three-dimensional sudden-contraction channel flows," *Phys. Rev. E.*, vol. 83, p. 046313, 2011.

[9] B. Semlitsch and M. Mihaescu, "Fluidic Injection Scenarios for Shock Pattern Manipulation in Exhausts," *Am. Inst. Astronaut. Aeronaut. J.*, vol. 56, no. 12, pp. 4640–4644, 2018.

[10] B. Semlitsch, D.M. Cuppoletti, E.J. Gutmark, and M. Mihaescu, "Transforming the Shock Pattern of Supersonic Jets Using Fluidic Injection," *Am. Inst. Astronaut. Aeronaut. J.*, vol. 576, no. 5, pp. 1851–1861, 2018.

[11] A.P. Khizar, P.S. Dabeer, and S.A. Khan, "Optimization of area ratio and thrust in suddenly expanded flow at supersonic Mach numbers," *Case Stud. Ther. Eng.*, vol. 12, pp. 696–700, 2018.

[12] A. Abid and S.A. Khan, "Investigation of high-speed flow control from C-D nozzle using design of experiments and CFD methods," *Arabian J Sci Eng.*, vol. 46, pp. 2201–2230, 2020.

[13] J.D. Quadros, S.A. Khan, A.J. Antony, and S.V. Jolene, "Experimental and Numerical Studies on Flow from Axisymmetric Nozzle Flow with Sudden Expansion for Mach 3.0 using CFD," *Int. J. Energy Environ. Econ.*, vol. 24, no. 1, pp. 61–72, 2016.

[14] J.D. Quadros and S.A. Khan, "Prediction of base pressure in a suddenly expanded flow process at supersonic Mach number regimes using ANN and CFD," *J Appl. Fluid. Mech.*, vol. 13, no. 2, pp. 499–511, 2020.

[15] R. Jagannath, N.G. Naresh, and K.M. Pandey, "Studies on Pressure Loss in Sudden Expansion in Flow through Nozzles: A Fuzzy Logic Approach," *ARPN J. Eng. Appl. Sci.*, vol. 2, pp. 50–61, 2007.

[16] A. Afzal, S.A. Khan, M.T. Islam, R.D. Jilte, A. Khan, and M.E.M. Soudagar, "Investigation and back-propagation modeling of base pressure at sonic and supersonic Mach numbers," *Phys. Fluids*, vol. 32, p. 096110, 2020.

[17] J.D. Quadros, S.A. Khan, S. Sapkota, J. Vikram, and T. Prashanth, "On Recirculation Region Length of Suddenly Expanded Supersonic Flows, Using CFD and Fuzzy Logic," *Int. J. Comput. Fluid Dyn.*, vol. 34, pp. 1–16, 2020.

[18] A. Afzal, A. Aabid, A. Khan, S.A. Khan, U. Rajak, T.N. Verma, and R. Kumar, "Response surface analysis, clustering, and random forest regression of pressure in suddenly expanded high-speed aerodynamic flows," *Aerosp. Sci. Technol.*, vol. 107, p. 106318, 2020.

10

Bull. Pol. Acad. Sci. Tech. Sci., vol. 70, no. 5, e142654, 2022

[19] A. Afzal and M.K. Ramis, "Multi-objective optimization of thermal performance in battery system using genetic and particle swarm algorithm combined with fuzzy logics," *J. Energy Storage*, vol. 32, p. 101815, 2020.

[20] A. Afzal, S. Alshahrani, A. Alrobaian, A. Buradi, and S.A. Khan, "Power Plant Energy Predictions Based on Thermal Factors Using Ridge and Support Vector Regressor Algorithms," *Energies*, vol. 14, no. 21, p. 7254, 2021.

[21] A. Afzal, J.K. Bhutto, A. Alrobaian, A. Razak Kaladgi, and S.A. Khan, "Modelling and Computational Experiment to Obtain Optimized Neural Network for Battery Thermal Management Data," *Energies*, vol. 14, no. 21, p. 7370, 2021.

[22] A. Afzal, K.M. Yashawantha, N. Aslfattahi, R. Saidur, R.K. Abdul Razak, and R. Subbiah, "Back propagation modelling of shear stress and viscosity of aqueous Ionic-MXene nanofluids," *J. Therm. Anal. Calorim.*, vol. 145, pp. 2129–2149, 2021.

[23] I. Mokashi, A. Afzal, S.A. Khan, N.A. Abdullah, M.H.B. Azami, R.D. Jilte, and O.D. Samuel, "Nusselt number analysis from a battery pack cooled by different fluids and multiple back-propagation modelling using feed-forward networks," *Int. J. Therm. Sci.*, vol. 161, p. 106738, 2021.

[24] J.D. Quadros, S.A. Khan, and A.J. Antony, "Modelling of Suddenly Expanded Flow Process in Supersonic Mach Regime using Design of Experiments and Response Surface Methodology," *J. Comput. Appl. Mech.*, vol. 49, no. 1, pp. 149–160, 2018.

[25] M.B. Parappagoudar, D.K. Pratihar, and G.L. Datta, "Linear and non-linear statistical modelling of green sand mould system," *Int. J. Cast Met. Res.*, vol. 20, no. 1, pp. 1–13, 2007.

[26] M.P.E. Gonzalez and L.E. García-Díaz, "Application of a Taguchi L_{16} orthogonal array for optimizing the removal of Acid Orange 8 using carbon with a low specific surface area," *Chem. Eng. J.*, vol. 163, no. 1–2, pp. 55–61, 2010.

[27] P.R. Vundavilli, M.B. Parappagoudar, S.P. Kodali, and S. Benguluri, "Fuzzy logic-based expert system for prediction of depth of cut in abrasive water jet machining process," *Knowledge Based Syst.*, vol. 27, pp. 456–464, 2012.

[28] B. Surekha, P.R. Vundavilli, and M.B. Parappagoudar, "Forward and reverse mappings of the cement-bonded sand mould system using fuzzy logic," *Int. J. Adv. Manufac. Technol.*, vol. 61, no. 9-12, pp. 843–854, 2012.

[29] M.G.C. Patel, P. Krishna, and M.B. Parappagoudar, "Prediction of Secondary Dendrite Arm Spacing in Squeeze Casting Using Fuzzy Logic Based Approaches," *Arch. Foundry Eng.*, vol. 15, no. 1, pp. 51–68, 2015.

[30] M.B. Parappagoudar and P.R. Vundavilli, "Application of modeling tools in manufacturing to improve quality and productivity with case study," *Proc. Manufac. Syst.*, vol. 7, no. 4, pp. 193–198, 2012.

[31] S. Haykin, *Neural networks: a comprehensive foundation*. Prentice Hall PTR, New Jersey, United States, 1994.

[32] S. Rajasekaran and G.V. Pai, *Neural networks, fuzzy logic and genetic algorithm: synthesis and applications*, PHI Learning Pvt. Ltd., India, 2003.

[33] B.K. Wong and V.S. Lai, "A survey of the application of fuzzy set theory in production and operations management: 1998–2009," *Int. J. Produc. Econom.*, vol. 129, no. 1, pp. 157–168, 2011.

[34] M.A. Yurdusev and M. Firat, "Adaptive neuro fuzzy inference system approach for municipal water consumption modeling: An application to Izmir, Turkey," *J. Hydrol.*, vol. 365, no. 3, pp. 225–234, 2009.

Bull. Pol. Acad. Sci. Tech. Sci., vol. 70, no. 5, p. e142654, 2022

11